Reciprocal Differentiation model of Th17 and iTreg

CPU CHINA iGEM 2017

October 31, 2017

1 Introduction

T helper cell (TH17) derives from nave CD4+ T cells. It can cells produce interleukin-17A (IL-17A), IL-17F and IL-22 as their lineage-defining cytokines, and the retinoic acid receptor-related orphan receptor gamma t (RORγt) transcription factor is considered the master regulator of this lineage. In addition, naive CD4 + T cells were found to be able to differentiate into a fourth lineage of (regulatory) T cells, which were called induced regulatory T (iTreg) cells. iTreg cells are characterized by producing IL-10 and transforming growth factor-b (TGF-β) and highly expressing forkhead box P3 (Foxp3) transcription factor as their master regulator. TH17 cells are pro-inflammatory because they secret cytokines that promote inflammation, whereas iTreg cells are anti-inflammatory because their lineage-defining cytokines can reduce the inflammatory response. Due to the different interation between them,we establish symmetrical and asymmetrical model to illustrate their function.

2 Modeling Procedure

2.1 Symmetrical mode

We constructed our mathematical model based on known interactions among key molecules in the differentiation system of TH17 and iTreg cells. For illustrative purposes, we first consider a symmetrical model in which the lineages of TH17 and iTreg have identical corresponding interaction types and strengths.

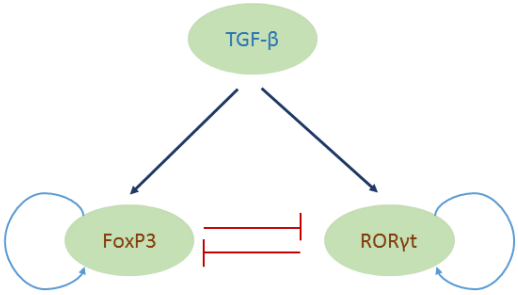

Figure 1: Symmetrical model without intermediates.

In the symmetrical model (Figure A), TGF-β upregulates both RORγt and Foxp3. The model includes the autoactivation of both master regulators. Although there is no evidence for direct autoactivation of RORγt and Foxp3, these relationships in our model represent known positive feedback loops in their respective pathways. One origin of these positive feedback loops is the epigenetic modifications observed in the promoter regions of RORγt and Foxp3 in their respective lineages. These epigenetic modifications recruit additional chromatin remodeling complexes that further stabilize those modifications and help to maintain the gene expression, thus forming positive feedback loops. Additionally, master regulators can enhance their own production by autocrine effects. The symmetric model also includes the cross-inhibition interactions between Foxp3 and RORγt. Inhibition of Foxp3 by RORγt is supported by the recent discovery that RORγt acts as a transcriptional repressor of Foxp3 by binding to its promoter. Although a few reports suggest a functional inhibition of RORγt by Foxp3, the presence of Foxp3 was shown to have no pronounced effect on the expression of RORγt. Our symmetrical model includes the inhibition of RORγt by Foxp3, but we relaxed this assumption in our model with broken symmetry.

on system, we use a generic form of ordinary differential equations (ODEs) that describe both gene expression and protein interaction networks. Each ODE in our model has the form:

$$\frac{dX}{dt} = \beta_i(F(\epsilon_i A_i)) - C_i \tag{1}$$

$$F(\epsilon W) = \frac{1}{1 + e^{-\epsilon W}} \tag{2}$$

$$W_i = \alpha_i^0 + \sum_j^n \alpha_{i->j} C_j \tag{3}$$

$$i = 1, ..., N \tag{4}$$

Xi is the activity or concentration of protein i. Xi(t) changes on a time scale =1/ci. Xi(t) relaxes toward a value determined by the sigmoidal function, F, which has a steepness set by si . The basal value of F, in the absence of any influencing factors, is determined by voi . The coefficients vj?i determine the influence of protein j on protein i. N is the total number of proteins in the network.

For example, the pair of ODEs for the first symmetrical model are:

$$\frac{d[ROR\gamma t]}{dt} = r_{ROR\gamma t}(\frac{1}{1 + e^{-\alpha_{ROR\gamma t} W_{ROR\gamma t}}} - [ROR\gamma t]) \tag{5}$$

$$W_{ROR\gamma t} = \alpha^0_{ROR\gamma t} + \alpha_{ROR\gamma t -> ROR\gamma t}[ROR\gamma t] + \alpha_{Foxp3 -> ROR\gamma t}[Foxp3] + \alpha_{TGF\beta -> ROR\gamma t}[TGF\beta] \tag{6}$$

$$\frac{d[Foxp3]}{dt} = rFoxp3(\frac{1}{1 + e^{-\alpha_{Foxp3} W_{Foxp3}}} - [Foxp3]) \tag{7}$$

$$W_{Foxp3} = \alpha^0_{Foxp3} + \alpha_{Foxp3 -> Foxp3}[Foxp3] + \alpha_{ROR\gamma t -> Foxp3}[ROR\gamma t] + \alpha_{TGF\beta -> Foxp3}[TGF\beta] \tag{8}$$

All variables and parameters are dimensionless. One time unit in our simulations corresponds to approximately 1 hour.

The solution of these ODEs for the basal values, and with [TGF-β] = 0, evolves to a stable steady state where both RORγt and Foxp3 have a low level of expression (RORγtlowFoxp3low). This steady state corresponds to a nave CD4 + T cell

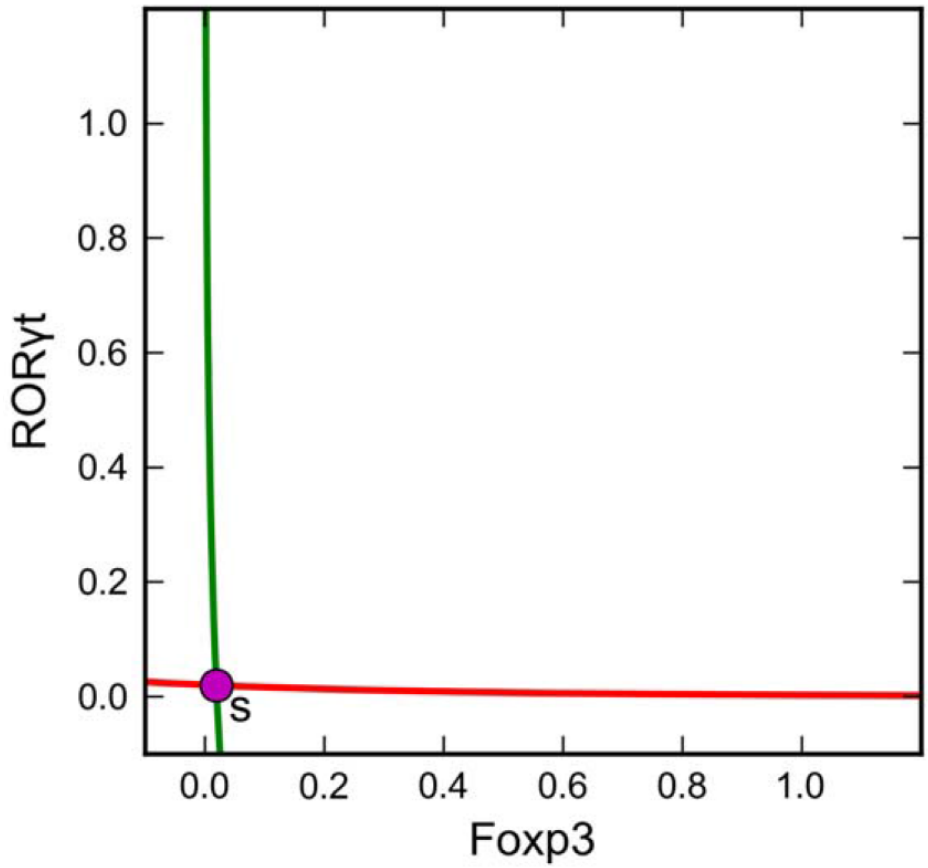

Figure 2: Phase plane for the average cell with $[TGF - \beta] = 0$

Figure 2 shows a scenario in which the TGF-β signal triggers the formation of a tri-stable system. In this particular case, the RORγtlowFoxp3 low state is no longer a stable steady state, and nave cell, which was previously stabilized in the RORγtlowFoxp3low state, would differentiate into the RORγthighFoxp3high state, whose basin of attraction (the white region in Figure 2) contains the nave state of the cell.

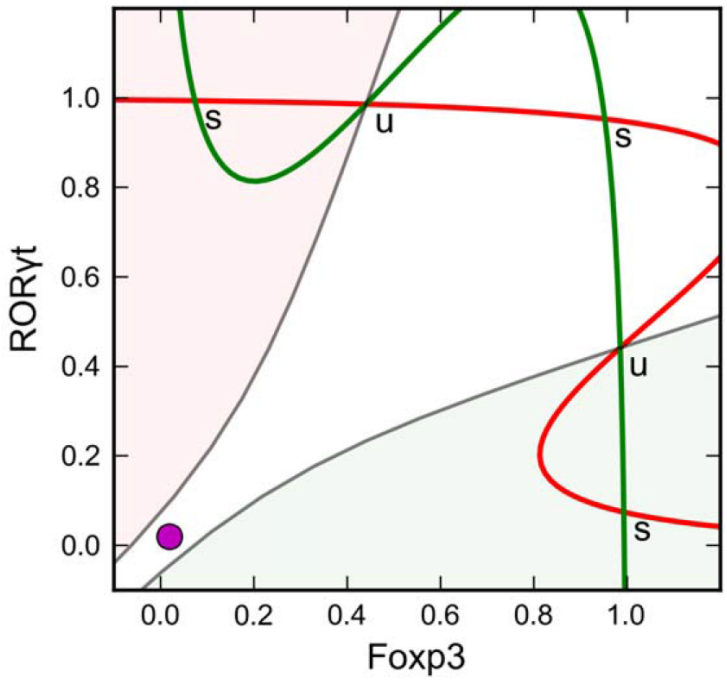

Figure 3: Phase plane for the average cell with $[TGF - \beta] = 0.5$ units.

However, cell-to-cell variability can produce other results. The basal settings correspond to the behavior of an average cell, but any particular cell will deviate somewhat from this average behavior. As consequences of the changing parameter values in any particular cell, the position of the RORγtlowFoxp3low state changes, the boundaries of the basins of attractions change, and the fate of the nave cell may change. Figure 3 depicts three cells in the population that adopt three different fates because of the variability among them. With a random sample of cells, each of the three differentiated states can be populated by a significant fraction of cells (Figure 4). Although cell-to-cell variability does not make large changes in the position of the lowFoxp3low state, it has a dramatic influence on the basins of attraction of the stable steady states, which determines the fate of the cell once the differentiation signal is turned on.

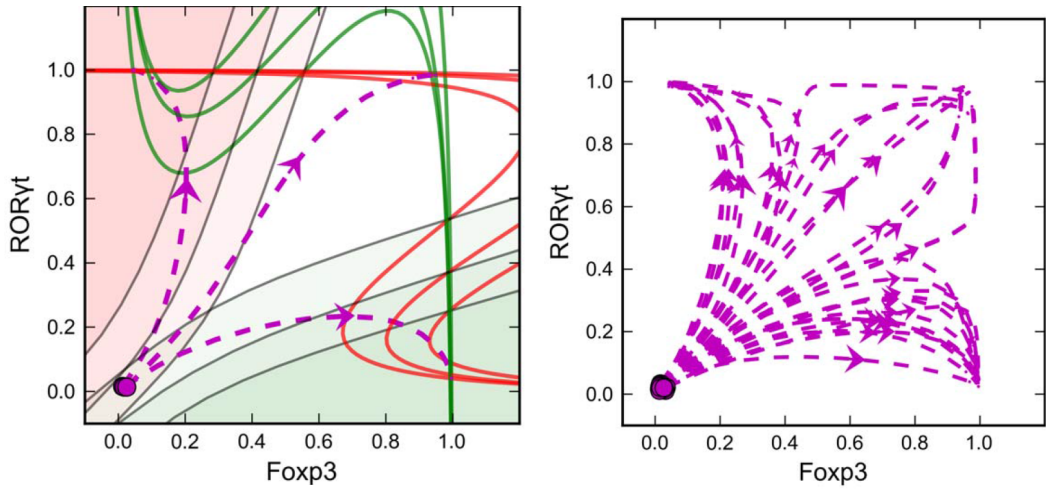

Figure 4: Overlaid phase planes and trajectories for three cells adopting distinct fates and Simulation trajectories for a population of 30 cells on the plane of $ROR\gamma t$ and Foxp3.

2.2 Asymmetrical model after adding two intermediate proteins

we added two intermediate proteins for transmitting TGF-β signals in this symmetrical model. And we modified our model so that it became asymmetrical, and we incorporated two other input signals.

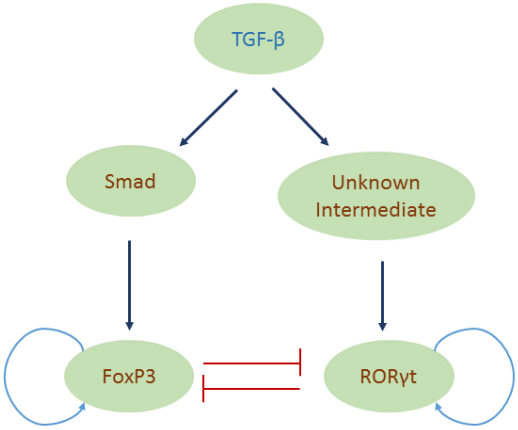

Figure 5: Symmetrical model with intermediates.

In this model, we added intermediate proteins between TGF-β and the master regulators. It is known that Smad2, Smad3 and Smad4 mediate the TGF-β induced upregulation of Foxp3, but the Smad proteins are dispensable for upregulation of RORγt. It is still unclear how the TGF-β signal is transmitted to RORγt. Thus, in Figure 1B, we introduce a generalized Smad intermediate between TGF-β and Foxp3 and an unknown intermediate between TGF-β and RORγt.

2.3 Asymmetrical model after adding external oscillation

The model with broken symmetry also includes IL-17, which is activated by RORγt and STAT3, and deactivated by Foxp3 and ATRA . As a polarizing signal, IL-6 stimulates RORγt and IL-17 production, and represses Foxp3 expression through the STAT3 pathway . Conversely, ATRA upregulates Foxp3, downregulates RORγt, and inhibits IL-17 production . These relations are all included in our model with broken symmetry.

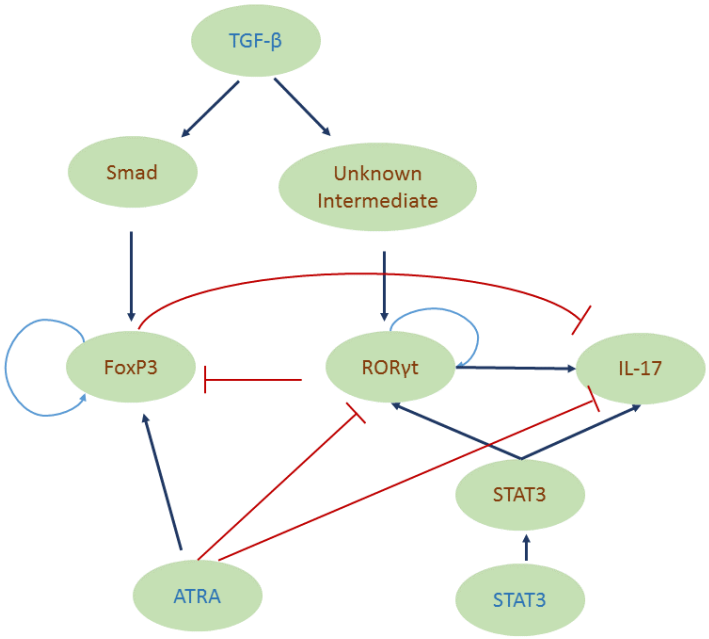

Figure 6: Asymmetrical model with three input signals: TGF-β, ATRA, and IL-6.

We next considered an asymmetrical model in which the network topology and parameter values differ from the symmetrical model. In the model with perfect symmetry, we assumed that the inhibitions between Foxp3 and RORγt are equally strong. Therefore, we revised our model by removing the direct inhibition of RORct expression by Foxp3 and adding the inhibition of IL-17 expression by Foxp3.

This revised model, with broken symmetry (Figure 1C, Table 1-last column, and Figure 3C) shows some new features. First, RORct behaves ultrasensitively in response to varying $[TGF-\beta]$ because of RORγt positive (autoregulatory) feedback loop. Secondly, Foxp3 exhibits multiple saddle-node bifurcations derived from the broken symmetries of the pitchforks. Interestingly, the four types of stable steady states observed with the symmetrical model have been retained for Foxp3, and thus for the entire system. In fact, by varying $[TGF-\beta]$, it is possible to obtain all three differentiated phenotypes in significant fractions simultaneously. At low $[TGF-\beta]$, Foxp3 singlepositive cells are predicted to be the dominant cell type. As $[TGF-\beta]$ increases to intermediate or high levels, the RORct singlepositive cells and the double-positive cells should appear and coexist.

Our model not only validates existing published data on the coexistence of two or more phenotypes in mixed T helper cell populations but also predicts that increasing TGF-b concentration will cause the transformation of Foxp3 single-positive cells into RORct-expressing cells. Conversely, decreasing TGF-b concentration might result in the reverse transformation.

3 Discussion

We have chosen to use generic (phenomenological) ODEs instead of a more detailed kinetic model of the biochemical reaction network because we lack sufficient mechanistic and kinetic information on the molecular interactions in the TH17-iTreg reciprocal-

differentiation system. To build a detailed biochemical model, based on mass-action or Michaelis-Menten kinetics, would require us to make many assumptions on the underlying mechanism and rate constants with little or no experimental evidence to back up these assumptions. In such a case, a phenomenological model seems more appropriate to us.

To account for cell-to-cell variability in a population, we made many simulations of the system of ODEs, each time with a slightly different choice of parameter values, to represent slight differences from cell to cell. We assumed that the value of each parameter conforms to a normal distribution with $CV = 0.05$ (CV = coefficient of variation = standard deviation/mean). The mean value that we specified for each parameter distribution is also referred as the basal value of that parameter (see Table 1). In our bifurcation analysis of the dynamical system, we consider an imaginary cell that adopts the basal value for each of its parameters, and we define this cell as the average cell. Note that none of the cells in our simulated population is likely to be this average cell, because every parameter value is likely to deviate a little ($CV = 5\%$) from the basal value. Note, in addition, that our simulations sample a volume of parameter space around the average cell, thereby probing the sensitivity/robustness of the differentiation process. Because we are varying all parameters simultaneously and randomly, this procedure is more indicative of robust behavior than standard sensitivity analysis, which involves estimating the partial derivative of some output property (e.g., steady state level of FoxP3) with respect to each parameter separately.

In order to simulate the induced differentiation process, we first solved the ODEs numerically with some small initial values of [RORγt] and [Foxp3] state and with $[TGF-\beta] = 0$ (and, if applicable, other input signals, e.g. IL-6 and ATRA, = 0 as well). After a short period of time, each simulated cell will find its own, stable $ROR\gamma t_{low} Foxp3_{low}$ steady state, corresponding to a naive CD4+ T cell. Next, we changed $[TGF - \beta]$ (and other input signals, if applicable) to a certain positive value and continued the numerical simulation. By the end of the simulation, each cell arrives at its corresponding induced phenotype, which might vary from cell to cell because of the parametric variability of the population. To simulate the reprogramming effect, the concentration of IL-6 was raised after the cells were stabilized in the differentiated state. We made the simple definition that a protein is expressed when its level is greater than 0.5 units.

Appendix

Table 1: Descriptions and basal values of parameters.

Parameter name	Description	Basal value in symmetrical model without intermediates	Basal value in symmetrical model with intermediates	Basal value in model with broken symmetry
$\gamma_{ROR\gamma t}$	Relaxation rate of $ROR\gamma t$	1	1	1
γ_{Foxp3}	Relaxation rate of Foxp3	1	1	1
$\sigma_{ROR\gamma t}$	Steepness of sigmoidal function for $ROR\gamma t$	5	5	7
σ_{Foxp3}	Steepness of sigmoidal function for Foxp3	5	5	5
$\omega^o_{ROR\gamma t}$	Basal activation state of $ROR\gamma t$	-0.8	-0.8	-0.84
ω^o_{Foxp3}	Basal activation state of Foxp3	-0.8	-0.8	-0.92
$\omega_{ROR\gamma t->ROR\gamma t}$	Weight of autoactivation of $ROR\Gamma T$	1.24	1.2	0.7
$\omega_{Foxp3->ROR\gamma t}$	Weight of inhibition on $ROR\gamma t$ by Foxp3	-0.4	-0.4	NA
$\omega_{Foxp3->Foxp3}$	Weight of autoactivation of Foxp3	1.24	1.24	1.28
$\omega_{ROR\gamma t->Foxp3}$	Weight of inhibition on Foxp3 by $ROR\gamma t$	-0.4	-0.4	-0.54
$\omega_{TGF-\beta->ROR\gamma t}$	Weight of activation on $OR\gamma t$ by $TGF-\beta$	1.2	NA	NA
$\omega_{TGF-\beta->Foxp3}$	Weight of activation on Foxp3 by $TGF-\beta$	1.2	NA	NA
γ_{UI}	Relaxation rate of unknown intermediate (UI)	NA	1	1
γ_{Smad}	Relaxation rate of Smad	NA	1	1
σ_{UI}	Steepness of sigmoidal function for UI	NA	10	12
σ_{Smad}	Steepness of sigmoidal function for Smad	NA	10	20
ω^o_{UI}	Basal activation state of UI	NA	-0.2	-0.23
ω^o_{Smad}	Basal activation state of Smad	NA	-0.2	-0.225
$\omega_{UI->ROR\gamma t}$	Weight of activation on $ROR\gamma t$ by UI	NA	0.62	0.86
$\omega_{Smad->Foxp3}$	Weight of activation on Foxp3 by Smad	NA	0.62	0.68
$\omega_{TGF-\beta->UI}$	Weight of activation on UI by $TGF-\beta$	NA	1.2	1
$\omega_{TGF-\beta->Smad}$	Weight of activation on Smad by $TGF-\beta$	NA	1.2	1
$\omega_{ATRA->ROR\gamma t}$	Weight of inhibition on $ROR\gamma t$ by ATRA	NA	NA	-0.04
$\omega_{ATRA->Foxp3}$	Weight of activation on Foxp3 by ATRA	NA	NA	0.035
γ_{IL17}	Relaxation rate of IL-17	NA	NA	1
σ_{IL17}	Steepness of sigmoidal function for IL-17	NA	NA	30
ω^o_{IL17}	Basal activation state of IL-17	NA	NA	-0.82
$\omega_{Foxp3->IL17}$	Weight of inhibition on IL-17 by Foxp3	NA	NA	-0.8
$\omega_{STAT3->IL17}$	Weight of activation on IL-17 by STAT3	NA	NA	0.6
$\omega_{ATRA->IL-17}$	Weight of inhibition on IL-17 by ATRA	NA	NA	-0.1
γ_{STAT3}	Relaxation rate of STAT3	NA	NA	0.1
σ_{STAT3}	Steepness of sigmoidal function for STAT3	NA	NA	10
ω^o_{STAT3}	Basal activation state of STAT3	NA	NA	-0.4
$\omega_{STAT3->ROR\gamma t}$	Weight of activation on $OR\gamma t$ by STAT3	NA	NA	0.2
$\omega_{STAT3->Foxp3}$	Weight of inhibition on Foxp3 by STAT3	NA	NA	-0.1
$\omega_{IL6->STAT3}$	Weight of activation on STAT3 by IL-6	NA	NA	0.6
$[IL6]$	Concentration of IL-6	NA	NA	C
$[ATRA]$	Concentration of ATRA	NA	NA	C
$[TGF-\beta]$	Concentration of $TGF-\beta$	C	C	C

References

[1] RH Clewley, WE Sherwood, MD LaMar, and JM Guckenheimer. Pydstool, a software environment for dynamical systems modeling. *URL http://pydstool. sourceforge. net*, 2007.

[2] Maria A Curotto de Lafaille, Nino Kutchukhidze, Shiqian Shen, Yi Ding, Herman Yee, and Juan J Lafaille. Adaptive foxp3+ regulatory t cell-dependent and-independent control of allergic inflammation. *Immunity*, 29(1):114–126, 2008.

[3] Marc A Gavin, Jeffrey P Rasmussen, Jason D Fontenot, Valeria Vasta, Vincent C Manganiello, Joseph A Beavo, and Alexander Y Rudensky. Foxp3-dependent programme of regulatory t-cell differentiation. *Nature*, 445(7129):771–775, 2007.

[4] Raúl Guantes and Juan F Poyatos. Multistable decision switches for flexible control of epigenetic differentiation. *PLoS computational biology*, 4(11):e1000235, 2008.

[5] Ivaylo I Ivanov, Brent S McKenzie, Liang Zhou, Carlos E Tadokoro, Alice Lepelley, Juan J Lafaille, Daniel J Cua, and Dan R Littman. The orphan nuclear receptor rorγt directs the differentiation program of proinflammatory il-17+ t helper cells. *Cell*, 126(6):1121–1133, 2006.

[6] Luca Mariani, Max Löhning, Andreas Radbruch, and Thomas Höfer. Transcriptional control networks of cell differentiation: insights from helper t lymphocytes. *Progress in biophysics and molecular biology*, 86(1):45–76, 2004.

[7] Mariana Esther Martinez-Sanchez, Luis Mendoza, Carlos Villarreal, and Elena R Alvarez-Buylla. A minimal regulatory network of extrinsic and intrinsic factors recovers observed patterns of cd4+ t cell differentiation and plasticity. *PLoS computational biology*, 11(6):e1004324, 2015.

[8] Luis Mendoza. A network model for the control of the differentiation process in th cells. *Biosystems*, 84(2):101–114, 2006.

[9] Luis Mendoza and Ioannis Xenarios. A method for the generation of standardized qualitative dynamical systems of regulatory networks. *Theoretical Biology and Medical Modelling*, 3(1):13, 2006.

[10] Kenneth M Murphy and Brigitta Stockinger. Effector t cell plasticity: flexibility in the face of changing circumstances. *Nature immunology*, 11(8):674–680, 2010.

[11] Aurélien Naldi, Jorge Carneiro, Claudine Chaouiya, and Denis Thieffry. Diversity and plasticity of th cell types predicted from regulatory network modelling. *PLoS computational biology*, 6(9):e1000912, 2010.

[12] Liang Zhou, Jared E Lopes, Mark MW Chong, Ivaylo I Ivanov, Roy Min, Gabriel D Victora, Yuelei Shen, Jianguang Du, Yuri P Rubtsov, Alexander Y Rudensky, et al. Tgf-β-induced foxp3 inhibits th17 cell differentiation by antagonizing rorγt function. *Nature*, 453(7192):236–240, 2008.

[13] Jinfang Zhu, Hidehiro Yamane, and William E Paul. Differentiation of effector cd4 t cell populations. *Annual review of immunology*, 28:445–489, 2009.